

# *In situ* measurement of the heat transfer coefficient on a building wall surface: *h*-measurement device based on a harmonic excitation

## Mesure *in situ* du coefficient d'échange sur une paroi de bâtiment : système basé sur une excitation harmonique

Adrien François<sup>1,2</sup>, Laurent Ibos<sup>1</sup>, Vincent Feuillet<sup>1</sup>, Johann Meulemans<sup>2</sup>

<sup>1</sup>Univ Paris Est Creteil, CERTES, F-94010 Creteil, France

<sup>2</sup>Saint-Gobain Research Paris, 39 quai Lucien Lefranc, F-93303 Aubervilliers Cedex

**ABSTRACT.** This paper presents a novel *in situ* measurement method of the total heat transfer coefficient on a building wall. The device developed is based on harmonic thermal load of the wall surface. *In situ* tests of the method were performed in a steady environment as well as in off-equilibrium conditions (generated using electrical heaters). The heat transfer coefficient was estimated to 7.5 and 9 W.m<sup>-2</sup>.K<sup>-1</sup> respectively. A parametric analysis allows determining the optimum operating conditions. The results obtained were in good agreement with standard values found in the literature. Measurement uncertainties were evaluated and a simple analytical model of the device was also developed.

**KEYWORDS.** *in situ*, measurements, heat transfer coefficient, harmonic, thermal quadrupoles, buildings.

### Nomenclature

#### Acronyms

HFM Heat Flux Meter  
MRT Mean Radiant Temperature  
TEC ThermoElectric Cooler

*h* heat transfer coefficient W.m<sup>-2</sup>.K<sup>-1</sup>  
*j* complex number such that  $j^2 = -1$   
*N* number of points  
*Nu* Nusselt number —  
*Pr* Prandtl number —  
*R* thermal resistance m<sup>2</sup>.K.W<sup>-1</sup>  
*Ra* Rayleigh number —  
 $\Re$  real part operator  
*T* temperature K  
*u* uncertainty  
*U* voltage V  
*Y* thermal admittance W.m<sup>-2</sup>.K<sup>-1</sup>

#### Greek symbols

$\beta$  expansion coefficient K<sup>-1</sup>  
 $\varepsilon$  surface emissivity —  
 $\zeta$  phase lag rad  
 $\lambda$  thermal conductivity W.m<sup>-1</sup>.K<sup>-1</sup>  
 $\nu$  cinematic viscosity m<sup>2</sup>.s<sup>-1</sup>  
 $\sigma$  Stefan-Boltzmann constant W.m<sup>-2</sup>.K<sup>-4</sup>  
 $\varphi$  heat flux density W.m<sup>-2</sup>

#### Roman Symbols

$A_1, B_1, C_1, D_1$  thermal quadrupole coefficients  
*a* thermal diffusivity m<sup>2</sup>.s<sup>-1</sup>  
*A* amplitude  
*C* heat capacity J.K<sup>-1</sup>  
*f* frequency s<sup>-1</sup>  
*g* gravity acceleration m<sup>2</sup>.s<sup>-1</sup>  
*FT* Fourier Transfer

#### Superscripts

— mean value  
~ complex harmonic  
^ estimated value

#### Subscripts

c convective  
op operative  
r radiative

## 1. Introduction

It has been shown that the uncertainties on the internal and external total heat exchange coefficients  $h_i$  and  $h_e$  (under the assumption of linearizable radiative heat transfers) have a large impact on building energy simulations (BES) outputs. These coefficients are also needed for an accurate *in situ* measurement of building heat losses. In both situations,  $h_i$  and  $h_e$  are seldom measured *in situ* because of the complexity of the process. Standard values [ISO6946] and empirical correlations [DEJ13] are rather used. While the former are often not adaptable to the situation experienced (specific geometry, wind speed, temperature gradient, etc.), the later are based on laboratory experiments which are usually not representative of conditions encountered in buildings. This makes the estimated values of  $h_i$  and  $h_e$  possibly highly inaccurate. Moreover, the uncertainties are rarely quantified.

Existing  $h$  measurement methods are usually only applicable in steady-state and are not able to capture temporal evolutions of the coefficient. In addition, they rely on the measurement of the so-called “operative” temperature (weighted average of the air and mean radiant temperatures). This temperature is complex to measure. It is usually supposed equal to the air temperature, which is not the case in many configurations, especially outdoor. Finally, the common approach consists in estimating the convective and radiative coefficients separately, so that the measurement uncertainties add up.

This paper proposes a novel *in situ* measurement method of the total heat exchange coefficient  $h$ . It is based on a periodic excitation. First, it is easy to implement and can be performed within only a few minutes. Second, it enables the continuous monitoring of the  $h$  coefficient, provided the variations of the environment temperature are not too fast (typically, the characteristic time of the variation should not be below one hour). Third, it does not require any knowledge of the operative temperature. This is interesting when the air temperature significantly differs from the mean radiant temperature. This happens in non-insulated buildings for example, or in dynamic regimes when the building is being heated up or cooled down rapidly. This novel measurement method is presented in a paper in the *Energy and Buildings* journal [FRA20]. The results presented here are additional information.

## 2. Presentation of the measurement method

### 2.1. Total heat transfer coefficient and operative temperature

The heat flux  $\varphi$  on the surface of a wall is given by (hypothesis of linearizable radiative hat flux):

$$\varphi = h_c (T - T_{\text{air}}) + h_r (T - T_{\text{MRT}}) \quad [1]$$

with  $h_c$  and  $h_r$  the convective and radiative heat transfer coefficients respectively,  $T$ ,  $T_{\text{air}}$  and  $T_{\text{MRT}}$  the surface, air and mean radiant temperatures respectively. The  $h_r$  coefficient is obtained from linearization of radiative heat transfers:

$$h_r = 4\varepsilon\sigma T_m^3 \quad [2]$$

with  $\varepsilon$  the wall emissivity,  $\sigma$  the Stefan-Boltzmann constant and  $T_m$  a mean temperature. As a first approximation,  $T_m = (T + T_{\text{MRT}}) / 2$ . It is usually not necessary to distinguish the radiative and convective components: the heat flux  $\varphi$  can be expressed as a function of the total heat transfer coefficient  $h$ . Equation 1 becomes:

$$\varphi = h (T - T_{\text{op}}) \quad [3]$$

with  $h = h_c + h_r$  and  $T_{\text{op}} = (h_c T_{\text{air}} + h_r T_{\text{MRT}}) / h$  the so-called operative temperature.

## 2.2. Device

The  $h$ -measurement method presented here is based on a sinusoidal thermal load. The " $h$ -meter" used is presented in Fig 1. It is made out of an array of nine thermoelectric coolers (TEC) sandwiched between two 1mm-thick aluminum plates to obtain a more uniform temperature. A 0.4 mm-thick heat flux meter (HFM) from Captec with a type-T thermocouple embedded inside is fixed on the face of this assembly in contact with the air. The surface of the  $h$ -meter is covered with an adhesive tape that has the same apparent emissivity than the wall on which the device is fixed: 0.94 (emissivities were measured between 2 and 20  $\mu\text{m}$  with an infrared spectrometer). As seen in Fig 2, the voltage  $U$  applied to the array of TEC is sinusoidal so that both the surface temperature and heat flux (given as variations around the mean value) are sinusoidal as well. It may be noted that the measurement noise on  $T$  and  $\varphi$  is very small.

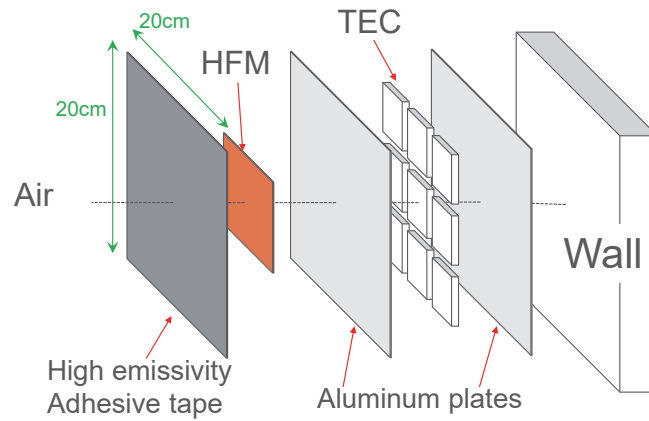


**Figure 1.** Scheme of the  $h$ -meter

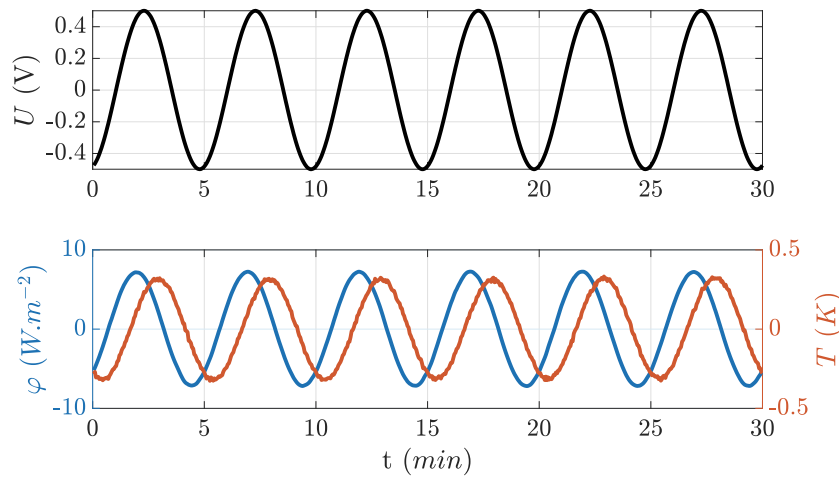


**Figure 2.** Input voltage (top) and measured surface heat flux and temperature variations (bottom)

## 2.3. Methodology

The operative temperature  $T_{\text{op}}$  is supposed to be constant for several oscillation periods. The temperature and heat flux are supposed measured exactly at the surface of the device. In the frequency domain (superscript  $\sim$  refers to complex harmonic notation), Eq 3 becomes:

$$\tilde{\varphi} = h\tilde{T} \quad [4]$$

where  $\tilde{\varphi} = \varphi - \bar{\varphi}$  with  $\bar{\varphi}$  the mean value during the few periods considered. Similarly for  $\tilde{T}$ . The estimated heat transfer coefficient  $\hat{h}$  is simply given by:

$$\hat{h} = \Re \left( \frac{\tilde{\varphi}}{\tilde{T}} \right) = \frac{A_\varphi}{A_T} \cos(\zeta) \quad [5]$$

with  $\Re$  the real part operator,  $A_\varphi$  and  $A_T$  the amplitudes of  $\varphi$  and  $T$  and  $\zeta$  the phase lag between them. In practice, the  $\hat{h}$  value is derived from the discrete Fourier transforms  $FT_T$  and  $FT_\varphi$  of the signals:

$$\hat{h} = \Re \left( \frac{FT_\varphi(k_f)}{FT_T(k_f)} \right) \quad [6]$$

with  $k_f$  the index of the harmonic corresponding to the excitation frequency  $f$ .

## 2.4. Measurement uncertainties

According to the GUM [GUM08], measurement uncertainties belong to two categories: type-A and type-B. Basically, type-A uncertainties are estimated by statistical methods whereas type-B ones are evaluated otherwise (they are not obtained from repeated observations). The Fourier transform of a  $N$ -point sequence  $y$  (measurements of  $T$  or  $\varphi$  for instance) for the index  $k_f$  is given by:

$$FT(k_f) = \frac{1}{N} \sum_{n=0}^{N-1} y(n) \exp\left(-j \frac{2\pi n}{N} k_f\right) = R + jI \quad [7]$$

with  $R$  and  $I$  the real and imaginary parts of  $FT(k_f)$ . The uncertainties over  $R$ ,  $I$  and the amplitude  $A = \sqrt{R^2 + I^2}$  are propagated from the uncertainties over  $y$  [BET00]:

$$u_R^2 = u_I^2 = u_A^2/4 = \frac{u_y^2}{2N} \quad [8]$$

The uncertainties over the amplitudes  $u_{A_\varphi}$  and  $u_{A_T}$  are estimated from the noise on the Fourier transforms of  $\varphi$  and  $T$ . Combining equations 6 and 7:

$$\hat{h} = \frac{R_\varphi R_T + I_\varphi I_T}{R_T^2 + I_T^2} \quad [9]$$

The propagation relates the uncertainty over the desired quantity  $\alpha$  to the  $m$  parameters  $\beta_1, \dots, \beta_m$  on which it depends:

$$u_\alpha = \sqrt{\sum_{i=1}^m \left( \frac{\partial \alpha}{\partial \beta_i} u_{\beta_i} \right)^2} \quad [10]$$

In the end, it comes:

$$u_{\hat{h}} = \frac{1}{A_T} \sqrt{u_{A_\varphi}^2 + \left( \frac{A_\varphi}{A_T} \right)^2 u_{A_T}^2} \quad [11]$$

Type-B uncertainties are propagated from sensors measurement uncertainties (thermocouple and heat flux meter).

### 3. Method optimization

The best operating conditions for the use of the "h-meter" were determined. Two parameters had to be adjusted: the period and the amplitude of the oscillations.

#### 3.1. Influence of the oscillation period

The oscillation period  $P$  was varied between 0.5 and 16 min during an experiment. The applied voltage and the operating conditions are kept constant. The measured heat flux and temperature are plotted in Fig 3. It may be noted that the higher  $P$ , the higher  $A_T$  and the smaller  $A_\varphi$ .

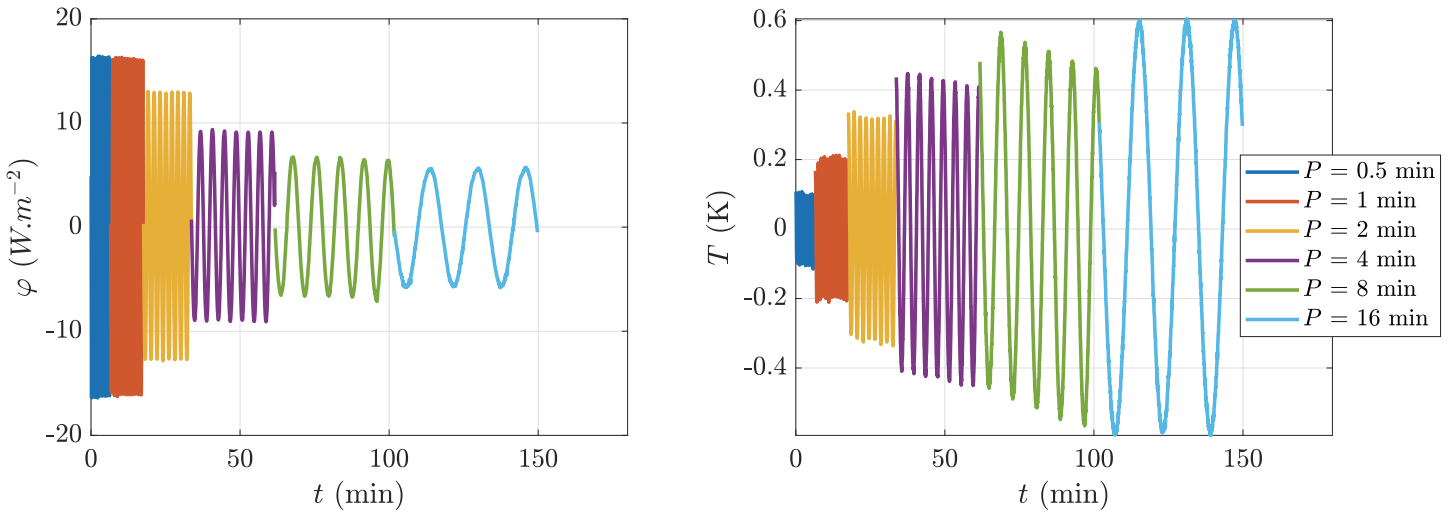


**Figure 3.** Measured heat flux (left) and temperature (right) on h-meter surface for several oscillation periods (variations around mean value)

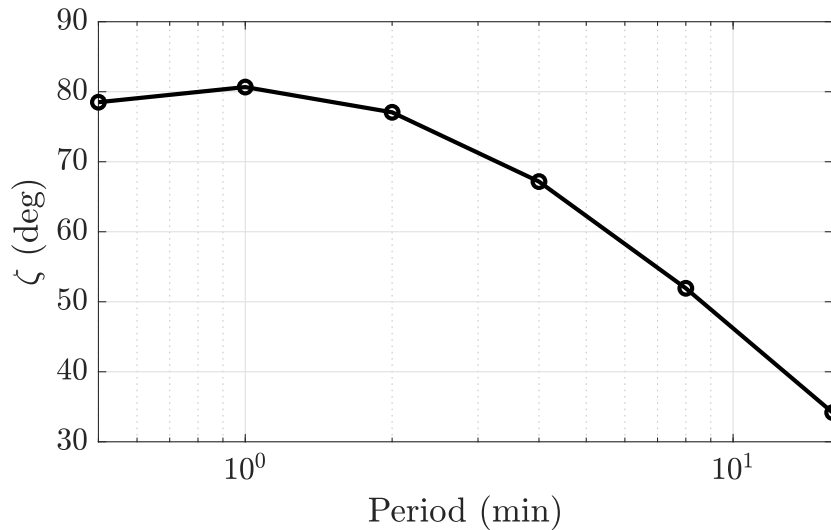


**Figure 4.** Influence of oscillation period on phase lag between  $\varphi$  and  $T$

In addition, as shown in Fig 4 the phase lag  $\zeta$  between  $\varphi$  and  $T$  increases as  $P$  decreases. At high frequencies,  $\zeta$  is even close to  $90^\circ$ . These observations are explained in more details in section 6. Finally, the impact of the period on the estimated heat transfer coefficient  $\hat{h}$  is presented in Fig 5.

Thus, a too short period leads to significant over-prediction of the  $h$ -value (a value around  $7.7 \text{ W} \cdot \text{m}^{-2} \cdot \text{K}^{-1}$  is expected [ISO6946]). This is mainly due to the thermal inertias of the HFM and the aluminum plate which are neglected in the model. At high frequency, these inertias have an impact on the phenomenon. On the other side, increasing the oscillation period above 5 min has almost no influence on the measured value. Therefore, the period of 5 min was retained.

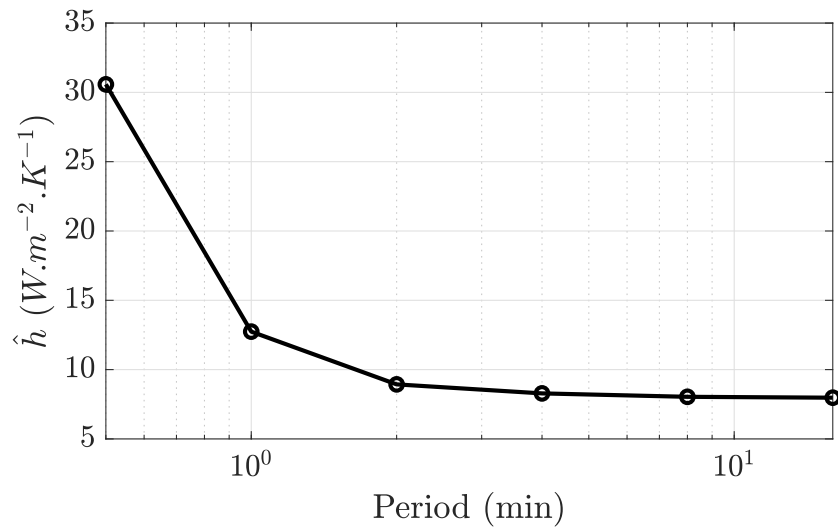


**Figure 5.** Influence of oscillation period on estimated  $h$ -value

### 3.2. Influence of the oscillation amplitude

To optimize the oscillation amplitude, the magnitude of the voltage supplied to the TEC was varied. Two configurations were tested: natural convection and forced convection. For the second one, a fan was used. The impact of the amplitude of temperature oscillations on the estimated heat transfer coefficient is visible in Fig 6. The experiments were repeated several times.

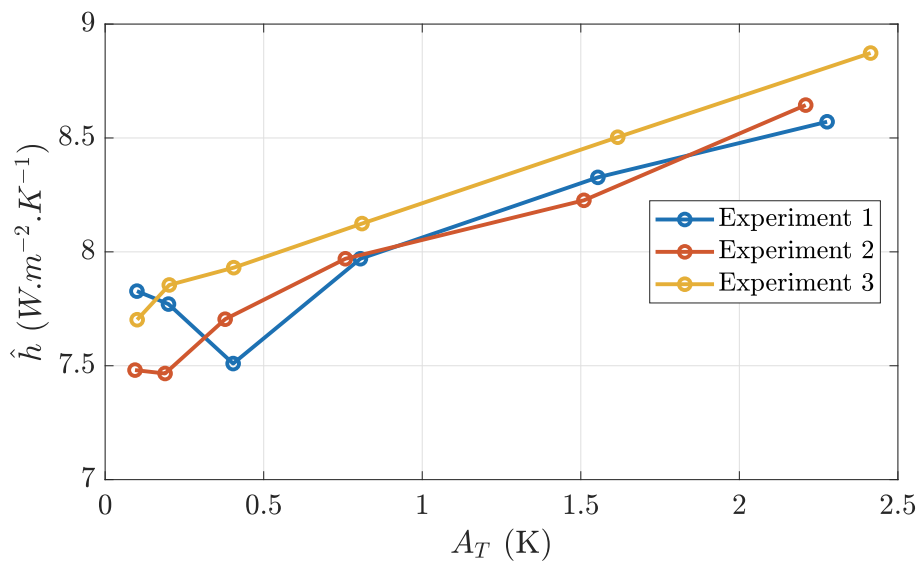


**Figure 6.** Measured  $h$ -coefficient according to the amplitude of temperature oscillations  $A_T$  in natural convection

In natural convection (Fig 7), the higher the temperature amplitude, the higher  $\hat{h}$ . This result is physical as in natural convection,  $h_c$  strongly depends on the temperature difference between the surface and the

fluid. Nevertheless, for the "*h*-meter" to be less intrusive as possible (do not locally change *h*),  $A_T$  should be small. It may be noted that  $\hat{h}$  is almost constant when  $A_T$  is below 0.5 K. In forced convection however,  $\hat{h}$  does not depend on the amplitude, which is also physical. Therefore, for the measurement to be accurate in any situation, the oscillations of the temperature should remain below 0.5 K.

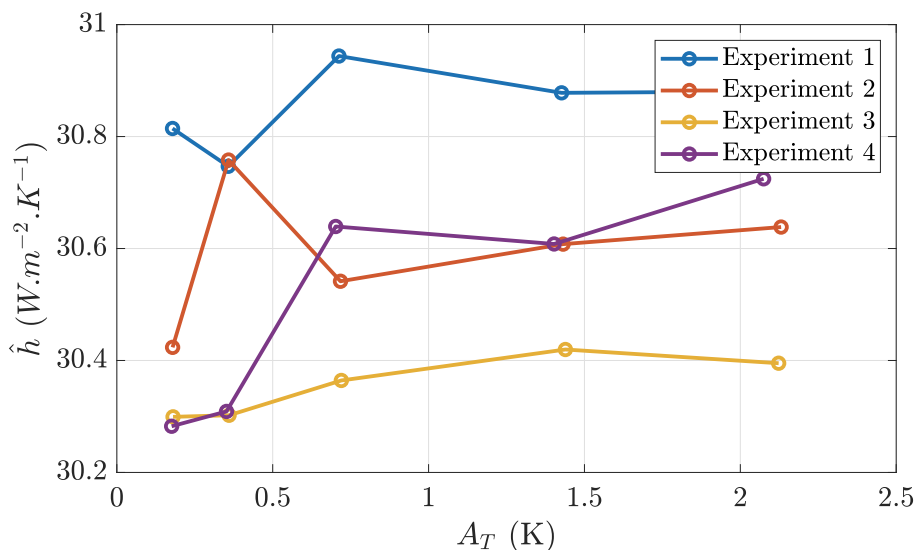


**Figure 7.** Measured *h*-coefficient according to the amplitude of temperature oscillations  $A_T$  in forces convection

#### 4. Experimental setup

The method was tested *in situ*. The *h*-meter was fixed 1.5 m high on the middle of a building interior wall. The windows were shut to prevent direct solar radiation. Each estimation was made from the analysis of six consecutive periods. Several numbers of periods were tested: six was chosen because it proved to minimize the measurement uncertainties. In order to generate off-equilibrium conditions, four 500 W electrical heaters were switched on for five hours and then switched off. Before the application of this thermal load, the room remained at thermal equilibrium for at least two days. Calibrated type-K thermocouples were used to measure air and wall temperatures. These measurements (made at the same altitude) are plotted in Fig 8 along with the temperature difference.

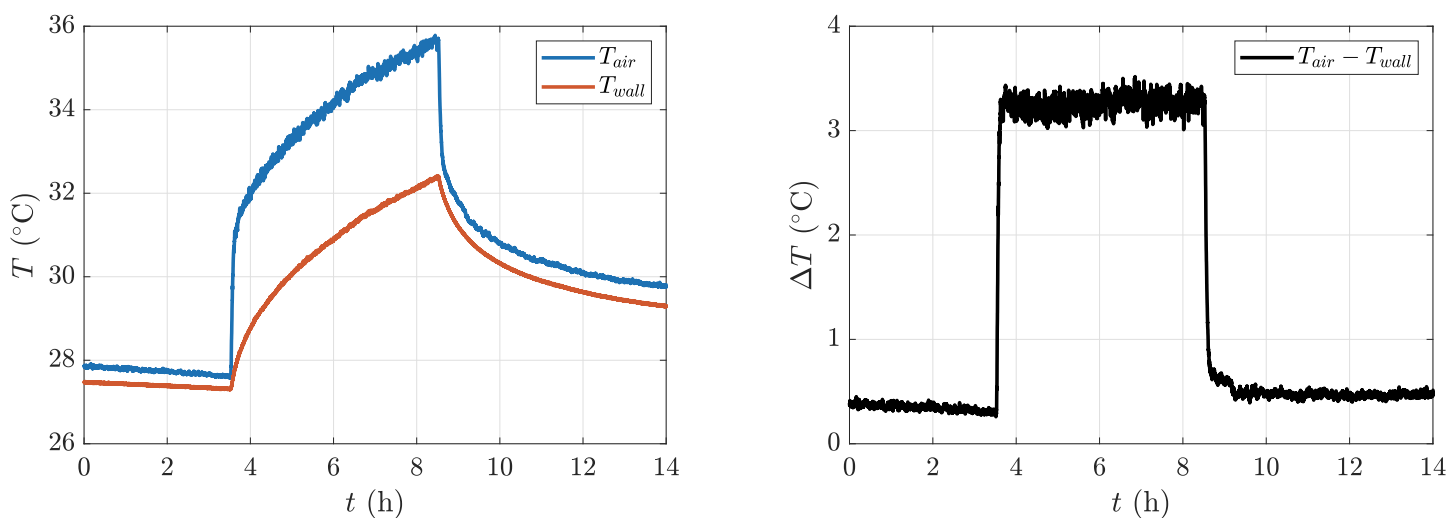


**Figure 8.** Indoor air and wall temperatures (left) and corresponding temperature difference (right)

It is important to point out that in this type of off-equilibrium situation, the usual assumption  $T_{op} = T_{air}$  is no longer valid. This is clearly visible in Fig 8 ( $T_{MRT}$  is supposed to be close to  $T_{wall}$ ). For this reason and also because of the air stratification, the use of  $T_{op}$  is complex, hence the advantage of our method that does not require  $T_{op}$ .

## 5. Results

The evolution of the measured heat transfer coefficient is plotted in Fig 9. Before and after the heating, the measured coefficient is between 7 and 7.5  $W.m^{-2}.K^{-1}$ . This is in good agreement with the standard value 7.7  $W.m^{-2}.K^{-1}$  from ISO 6946 [ISO6946]. During the heating phase however,  $\hat{h}$  is larger (around 9  $W.m^{-2}.K^{-1}$ ), as so is its variance and uncertainty. This may be explained by the air movements induced by the heaters which changed the convection environment. The measurement uncertainty is around 0.5  $W.m^{-2}.K^{-1}$ .

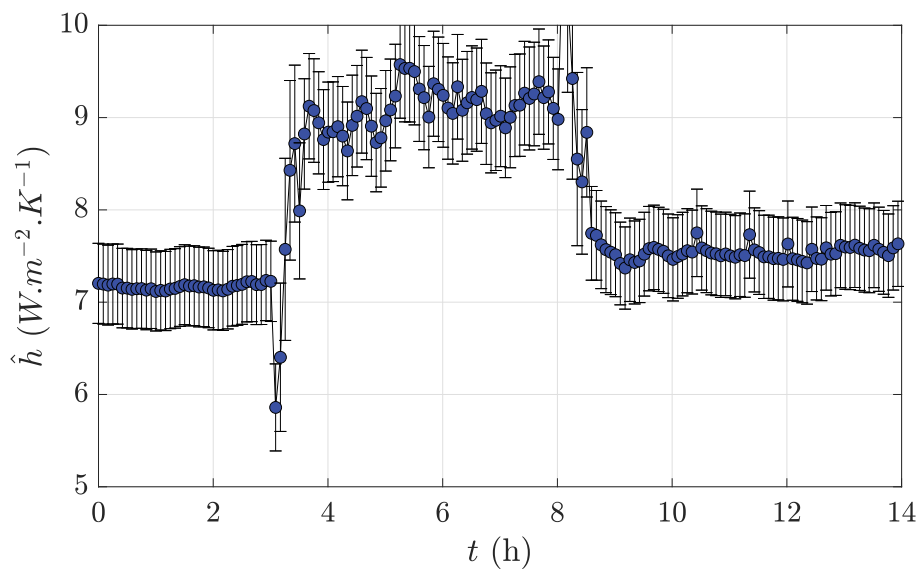


**Figure 9.** Measured  $h$ -value with uncertainties

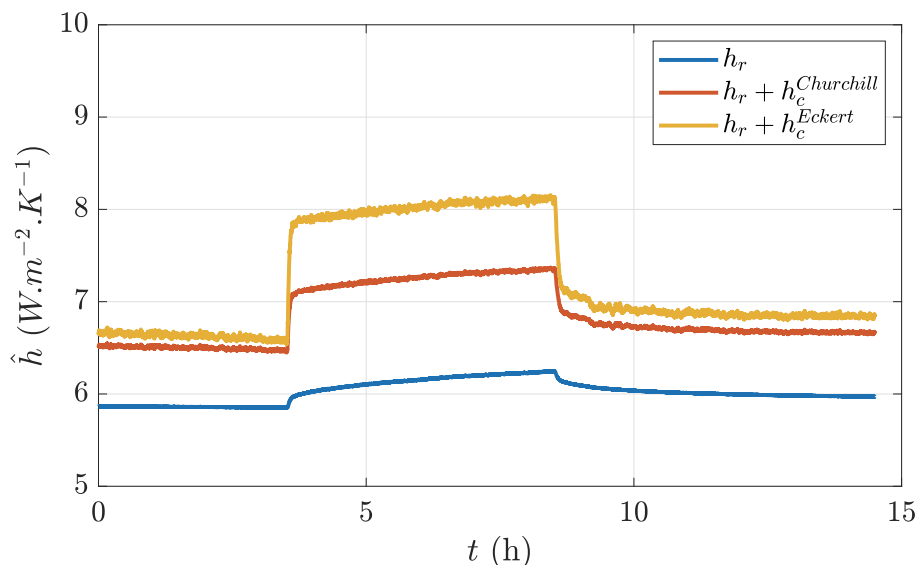


**Figure 10.** Estimated  $h$ -value from empirical correlations

The measurements are compared to predictions from two empirical correlations of  $h_c$  for vertical natural convection problems from the literature:

$$Nu_x = 0.0295 \frac{Pr^{1/15}}{(1 + 0.494Pr^{2/3})^{2/5}} Ra_x^{2/5} \quad [12]$$

$$Nu_x = 0.68 + \frac{3}{4} \times 0.515 \times Ra_x^{1/4} \quad [13]$$

with  $Nu_x = \frac{h_c \cdot x}{\lambda}$ ,  $Pr = \frac{\nu}{a}$ ,  $Ra = \frac{g \cdot \beta \cdot \Delta T \cdot x^3}{\nu^2} Pr$ , respectively the Nusselt, Prandtl and Rayleigh numbers,  $x$  the characteristic dimension of the problem (here the altitude),  $\nu$ ,  $a$  and  $\lambda$  are the air cinematic viscosity, thermal diffusivity and thermal conductivity respectively,  $g$  the gravity acceleration,  $\beta = 1/T_{air}$  the air expansion coefficient and  $\Delta T = T_{air} - T_{wall}$ . The combination of measured temperatures (see Fig 8), equations 12, 13 (for  $h_c$ ) and 2 (for  $h_r$ ) lead to the estimated  $\hat{h}$ -value plotted in Fig 10. It may be noticed that the two tested correlations both under-predict  $h$  but also give results that are very different from each other. This is an illustration of the limitations of empirical correlations: they were developed in laboratory conditions that are not always representative of *in situ* conditions. In particular, the air movements induced by the heaters probably turns the natural convection into mixed convection.

For further validation, the present measurement method was compared to other measurement methods for the quantification of the global heat transfer coefficient [FRA20]. A very good agreement between the methods was obtained.

## 6. Theoretical model

In order to justify some of the tendencies observed, a simple analytical model of the  $h$ -meter was developed. Basically, the measured temperature and heat flux are not exactly the one on the surface of the device. Indeed, the HFM is located below some adhesive tape (useful to increase its emissivity) and the HFM itself is covered with a copper sheet. These layers introduce a bias in the measurement of surface quantities despite their very small thicknesses. As shown in Fig 11, they are modeled here as a unique layer of thermal resistance  $R$  and capacity  $C$ .

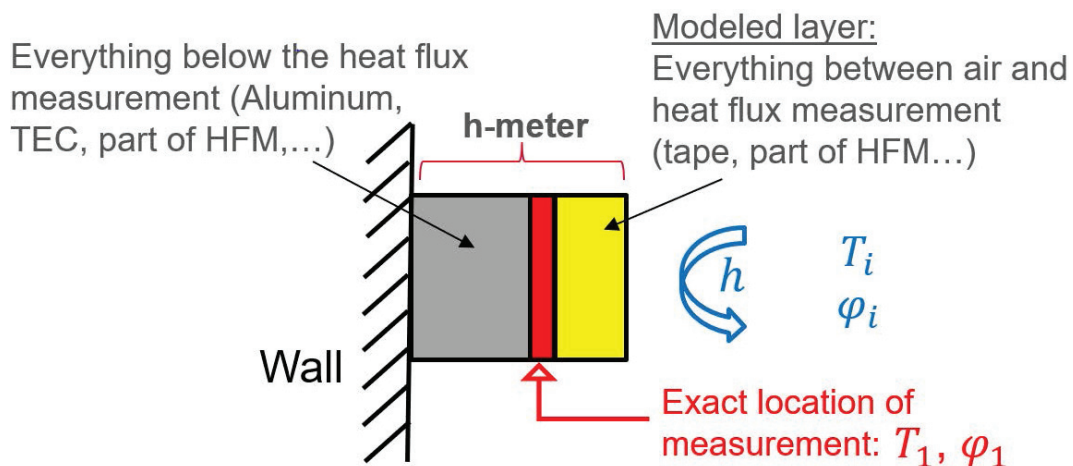


**Figure 11.** Simplified scheme of the  $h$ -meter

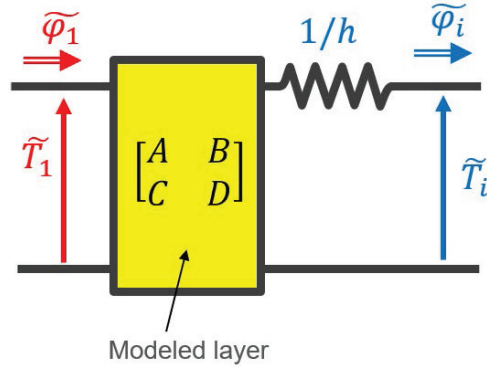


**Figure 12.** Electrical analogy of the modeled layer

The problem is modeled in the frequency domain with the thermal quadrupole formalism [MAI13] (see electrical analogy in Fig 12):

$$\begin{bmatrix} \tilde{T}_1 \\ \tilde{\varphi}_1 \end{bmatrix} = \begin{bmatrix} A_1 & B_1 \\ C_1 & D_1 \end{bmatrix} \times \begin{bmatrix} 1 & 1/h \\ 0 & 1 \end{bmatrix} \times \begin{bmatrix} \tilde{T}_i \\ \tilde{\varphi}_i \end{bmatrix} \quad [14]$$

with

$$\begin{bmatrix} A_1 & B_1 \\ C_1 & D_1 \end{bmatrix} = \begin{bmatrix} \cosh(\sqrt{i2\pi fRC}) & \sinh(\sqrt{i2\pi fRC}) / \sqrt{i2\pi fC/R} \\ \sinh(\sqrt{i2\pi fRC}) \times \sqrt{i2\pi fC/R} & \cosh(\sqrt{i2\pi fRC}) \end{bmatrix} \quad [15]$$

The cut-off frequency  $1/(RC)$  was roughly estimated to 3 Hz (for 0.2 mm of adhesive tape of thermal conductivity  $0.1 \text{ W}\cdot\text{m}^{-1}\cdot\text{K}^{-1}$  and diffusivity  $0.13 \times 10^{-6} \text{ m}^2\cdot\text{s}^{-1}$ ) which is three orders of magnitude above the oscillation frequency. Then, Eq 15 is simplified to:

$$\begin{bmatrix} A_1 & B_1 \\ C_1 & D_1 \end{bmatrix} \xrightarrow{f \rightarrow 0} \begin{bmatrix} 1 & R \\ i2\pi fC & 1 \end{bmatrix} \quad [16]$$

The indoor air temperature is supposed constant:  $\tilde{T}_i = 0$ . It comes the admittance:

$$Y = \frac{\tilde{\varphi}_1}{\tilde{T}_1} = \frac{D_1 h + C_1}{A_1 + hB_1} \xrightarrow{f \rightarrow 0} \frac{h + i2\pi fC}{1 + hR} \quad [17]$$

Hence

$$\|Y\| \simeq \frac{\sqrt{h^2 + 4\pi^2 f^2 C^2}}{1 + hR} \quad [18]$$

$$\zeta \simeq \text{atan} \left( \frac{2\pi fC}{h} \right) \quad [19]$$

and, given that  $hR \ll 1$ :

$$\hat{h} = \Re(Y) \simeq \frac{h}{1 + hR} \simeq h - h^2 R \quad [20]$$

Eq 19 proves that the phase lag  $\zeta$  between the measured quantities  $T_1$  and  $\varphi_1$  increases with the oscillation frequency, and therefore decreases with the period, as noted in Fig 4. As seen in Eq 20, the thermal resistance  $R$  of the small layer between the measurement location and the air introduces a negative bias on  $\hat{h}$  that increases linearly with  $R$  and quadratically with  $h$ . Eq 18 shows that the higher thermal capacity  $C$  of the layer, the higher  $\|Y\| = A_\varphi/A_T$  which increases the measurement uncertainties (see Eq 11).

## 7. Conclusion

The total heat transfer coefficient  $h$  on a building wall is seldom measured *in situ*. Yet, its value has a major impact on building energy simulations and on *in situ* thermal losses quantifications. The present work proposes an *in situ* measurement method of  $h$  based on a harmonic excitation. A " $h$ -meter", mainly made of thermoelectric coolers and a heat flux meter, was developed and implemented on an indoor wall. The optimal operating conditions (period and amplitude of the oscillations) were determined thanks to a parametric analysis. The method was validated in laboratory on test cases both in steady-state and off-equilibrium conditions (four 500 W electrical heaters heated up the indoor air). The heat transfer coefficient was estimated to  $7.5 \text{ W}\cdot\text{m}^{-2}\cdot\text{K}^{-1}$  for the state-state case and  $9 \text{ W}\cdot\text{m}^{-2}\cdot\text{K}^{-1}$  for the heating case. The technique proved a good reproducibility and agrees well in steady-state with standard value from ISO 6946 [ISO6946]. Some discrepancies are observed with empirical correlations from the literature, mainly because they were derived from experiments not representative of building conditions. The measurement uncertainty was estimated around  $0.5 \text{ W}\cdot\text{m}^{-2}\cdot\text{K}^{-1}$ . In future work, it would be interesting to test the methodology outdoor and to investigate the impact of changing the emissivity of the device.

## References

- [ISO6946] EN ISO 6946, *Building components and building elements-Thermal resistance and thermal transmittance-Calculation method*, 2007.
- [BEJ13] BEJAN A. , *Convection heat transfer*, John Wiley & Sons, 2013.
- [FRA20] FRANÇOIS A., IBOS L., FEUILLET V., MEULEMANS J., Novel *in situ* measurement methods of the total heat transfer coefficient on building walls, *Energy and Buildings*, 219:110004, 2020.
- [GUM08] IEC BIPM, ILAC IFCC, IUPAC ISO, *Guide to the expression of uncertainty in measurement (GUM: 1995 with minor corrections)* bureau international des poids et mesures, 2008.
- [BET00] BETTA G., LIGUORI C., PIETROSANTO A., Propagation of uncertainty in a discrete Fourier transform algorithm, *Measurement*, 27 (2000) 231-239.
- [TAI14] TAINÉ J., ENGUEHARD F., IACONA E., *Transferts thermiques-Introduction aux transferts d'énergie- 5e édition*, Dunod, 2014.
- [MAI13] MAILLET D., ANDRÉ S., BATSALE J.C., DEGIOVANNI A., MOYNE C., *Thermal quadrupoles: solving the heat equation through integral transforms*, John Wiley & Sons Inc, 2013.